



RC structural damages observed after October 30, 2020, Seferihisar—İZMİR earthquake and analytical evaluation of existing sample RC buildings

M. Koçer¹ · A. Ünal¹

Received: 18 December 2021 / Accepted: 7 February 2023 / Published online: 19 February 2023
© The Author(s), under exclusive licence to Springer Nature B.V. 2023

Abstract

In Turkey, the İzmir earthquake with $M_w=6.9$ moment magnitude with the epicenter of 17.26 km off the Seferihisar (İzmir) coast in the Aegean Sea occurred in October 30, 2020, at Turkish time 14.51. According to the acceleration records of İzmir earthquake, the recorded peak ground acceleration (PGA) was approximately 0.182 g, and 117 deaths occurred in this earthquake, while 1032 people were injured. In this study, the structural damages that occurred on the buildings due to the İzmir earthquake were examined and discussed in detail according to the current and former Turkish regulations. Moreover, a RC building constructed in 1998 and survived the earthquake without any permanent damage (a 5-story building designed as 3-story in the existing static project but added two more floors without any in situ strengthening) was subjected to pushover analysis, linear analyses considering regulations and nonlinear time-history pushover analysis according to the acceleration records of İzmir earthquake. The obtained structural results were compared and discussed according to the current and former regulations.

Keywords Earthquake damages · Failure types · Turkish building code · Nonlinear time-history analysis · Pushover analysis

1 Introduction

Turkey, one of the countries with the highest seismicity, is located in the Alpine–Himalayan seismic belt, which is active, and on which 20 percent of the earthquakes on the world occur and cause a destructive earthquake in Turkey in every 5 years (Fig. 1) (AFAD 2021). According to the Turkish Earthquake Code 2018 (TEC 2018), approximately 95% of Turkey's population lives under earthquake risk. Many destructive earthquakes occurred in Turkey in recent 30 years (Erzincan Earthquake in 1992, $M_w=6.8$; Adana-Ceyhan Earthquake in 1996, $M_w=6.3$; Adapazarı–İzmit Earthquake in 1999, $M_w=7.4$; Düzce Earthquake in 1999, $M_w=7.2$; Afyon–Sultandağı Earthquake in 2002, $M_w=6.5$; Bingöl Earthquake in

✉ M. Koçer
mkocer@ktun.edu.tr

¹ Department of Civil Engineering, Konya Technical University, Konya, Türkiye

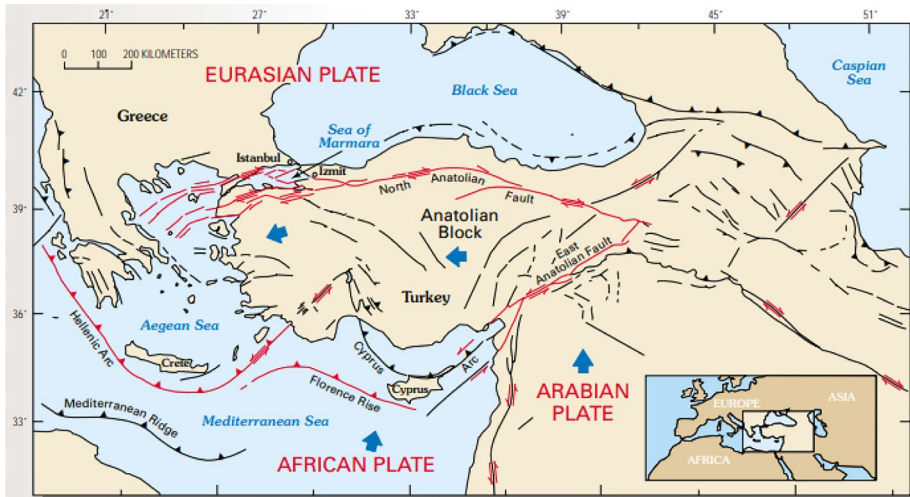


Fig. 1 The impact of Alpine–Himalayan Seismic Belt on Turkey (Sezen et al. 2003)

2003, $M_w=6.4$; Elazığ Earthquake in 2010, $M_w=6.0$; Van Earthquake in 2011, $M_w=7.2$; Simav Earthquake in 2011, $M_w=5.7$; Sivrice Earthquake in 2019, $M_w=5.2$) (AFAD 2021; Arslan and Korkmaz 2007; Murat 2015; Arslan et al. 2013; Yurdakul et al. 2020; Çağatay 2005; Inel et al. 2008; Tan et al. 2008; Adalier 2001; Sezen et al. 2003; Doğangün 2004; Kaplan et al. 2004; Gross and J. L., Phan 2000) (Fig. 2).

Reinforced concrete structures in Turkey generally consist of frames with insufficient lateral strength and stiffness, inadequate reinforcement details in terms of earthquake behavior, and low concrete strength. In addition, the presence of system inadequacies such as soft floors, short columns, strong beams and weak columns in these structures raises a large building stock with insufficient earthquake safety. It is not possible to expect structures with these weaknesses to exhibit healthy behavior in a strong earthquake (Kaplan

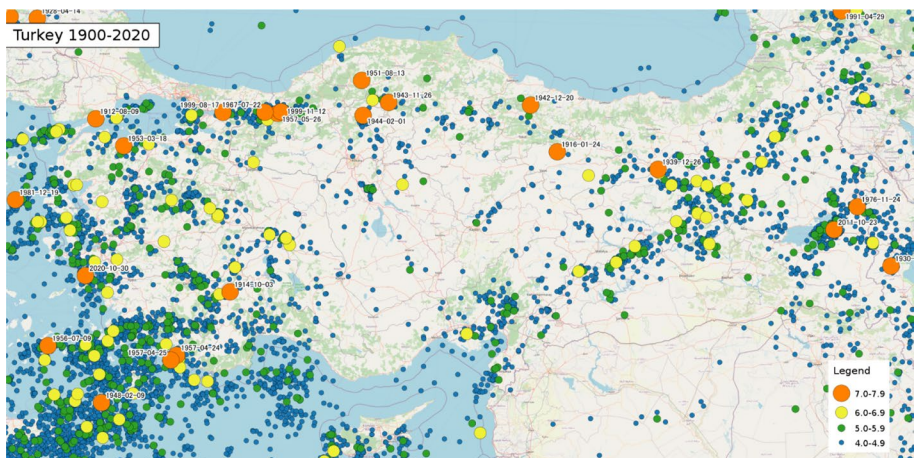


Fig. 2 Major earthquakes in Turkey in the last 30 years (AFAD 2021)

et al. 2004; Shendkar et al. 2022; Ulusay et al. 2012). The identification of the earthquake hazard and the determination of the vulnerability of building systems are the two main components of the studies carried out to predict the impact of earthquake disasters. The latter aims at the preparation of a micro-zoning map and is beyond the scope of this study. However, in the preparation phase of disaster scenarios, the issues specific to the building stock in our country should be taken into consideration while determining the vulnerability curves of the buildings. There are studies in the literature on damage observation and vulnerability assessments before and after an earthquake and how these assessments can be optimized based on observations and lessons learned (Işık et al. 2020; Chaoxu et al. 2021; Buyuksarac et al. 2021). In Turkey, a large database has been created on the damage observed after earthquakes, especially in recent years. The most important point here is that the data on the structures where damage was observed were taken meticulously, taking into account that it will be used in a statistical study later (AFAD 2021).

The first seismic hazard map of Turkey was prepared in 1945 as the Turkey Earthquake Zone Map and has been updated many times until today (Akkar et al. 2018a). Turkey Earthquake Zone Map has been prepared based on the peak ground acceleration (PGA) values of 475 years and the recommended acceleration ranges (Gülkan et al. 1993). In this map, the earthquake hazard is graded from 1 to 5 and the map is divided into five different earthquake zones. The same effective ground acceleration coefficient is proposed for each region. The effective ground acceleration coefficient takes the values of 0.4, 0.3, 0.2 and 0.1 for the 1st, 2nd, 3rd and 4th degree earthquake zones, respectively (α). This map came into effect in 1996 and is known as the Turkey Earthquake Zone Map. In the regulation that came into force in 2019, Turkey Earthquake Hazard Map was started to be used instead of earthquake zones. Site-specific seismic hazard assessment is the main advantage of the new seismic code. In general, in this code, seismicity elements, faults and fault groups in the region, characteristics of the faults, distance of the structure to the faults, the studied region and the characteristics of the earthquakes are taken into consideration (AFAD 2021; Akkar et al. 2014, 2018a, 2018b).

More than 500,000 buildings have been destroyed and thousands of people died due to the destructive earthquakes occurred in Turkey in the last century. According to the data of the Health Disaster Coordination Center (SAKOM), 117 people lost their lives in the İzmir earthquake and 1032 people were injured (SAKOM 2020). As a result of the damage assessment studies carried out by AFAD after the earthquake, it was determined that 17 of buildings have been collapsed, 506 of buildings had severe damages, 511 of buildings had intermediate damages, 5119 of buildings had light damages, and the number of buildings having no damage was 103,785 (AFAD 2021).

The last destructive earthquake in Turkey occurred on October 30, 2020, at 14:51 Turkish time with the epicenter of Aegean Sea, 17.26 km off the Seferihisar (İzmir) coast. The magnitude of the earthquake was announced as 6.9 M_w by Kandilli Observatory (RETMC, Regional Earthquake-Tsunami Monitoring Center (RETMC) 2021), 6.6 M_w by Disaster and Emergency Management Presidency (AFAD) (AFAD 2021), 6.7 M_L by Athens Geodynamic Institute (NOA 2021), 7.0 M_w by United States Geological Survey (USGS) (USGS 2021) and European-Mediterranean Seismological Center (EMSC) (EMSC 2021). In Fig. 3, the epicenter, the focal depth and the rapid moment tensor solutions proposed by the national and international seismology centers for the Aegean Sea Earthquake occurred in 30 October, 2020, are displayed. In addition, a small-scale tsunami occurred as a result of the earthquake.

One of the main purposes of this study, briefly, is to examine the structural damages in buildings due to the Izmir earthquake. Depending on the updates in the building codes, these

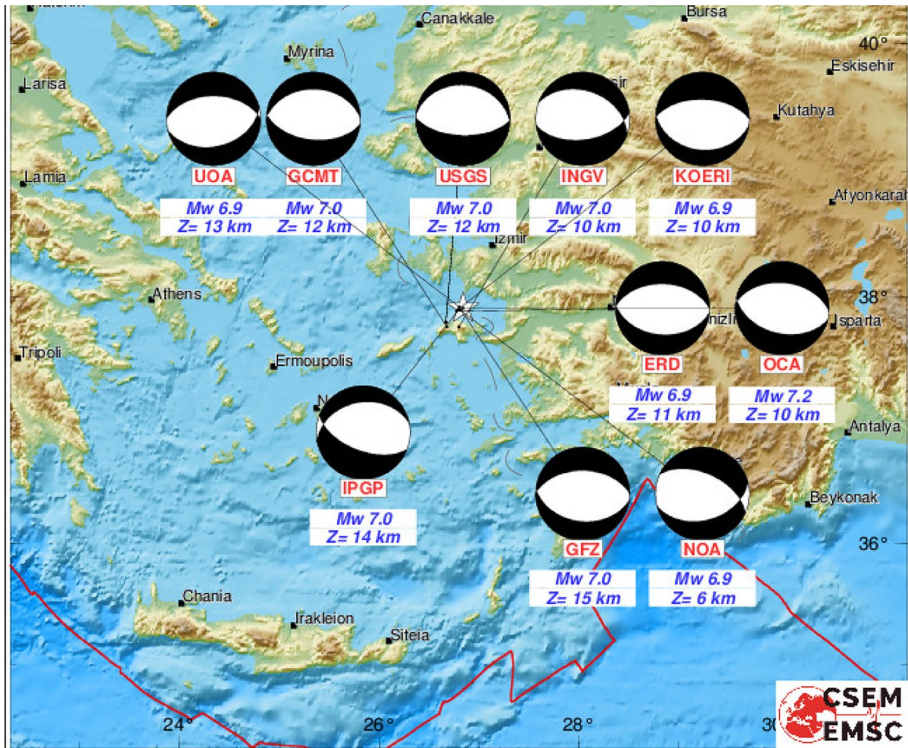


Fig. 3 Focal depth and rapid moment tensor solutions of different seismology centers for the İzmir Earthquake (EMSC 2021)

structural damage types have been critically examined and discussed according to the current and former Turkish codes. Another main objective of this study is to perform linear and nonlinear analyses on a 5-story building, which was designed as 3-story in the existing static project but two more floors were added without in situ retrofitting and survived the earthquake without structural damage. Linear analyses were carried out on this building, both in the year of construction and in accordance with the design spectrum of the current regulations, as both 3 and 5 floors. Then, nonlinear time-history pushover analysis and static pushover analysis were performed according to the İzmir earthquake acceleration records. The originality of this study is the comparison of analytical and observational earthquake damages by performing nonlinear time-history pushover analysis according to the İzmir earthquake acceleration record on a structure exposed to the İzmir earthquake. The structural results obtained were compared according to the current and old regulations, and the results were interpreted.

2 Geological features of the region

2.1 Tectonic Features of the Region

İzmir City is located at the western end of the Gediz Graben system under the effect of Western Anatolia Extensional Regime. The normal faulting in the E–W direction takes

place at the western end of the Gediz Graben, especially NE–SW and NW–SE faults are concentrated around İzmir City. Apart from the Gediz Graben, the active faults that can cause an earthquake activity at the region are Tuzla, Seferihisar, Gülbahçe, Mordağan, Gümüdür, İzmir, Menemen, Güzelhisar, Yeni Foça and Kiraz faults (Fig. 4). During the Instrumental Period (A.D. 1900–2019; magnitude $M > 4.0$), the magnitudes of the significant earthquakes that occurred inside the city borders are between $M = 7.0$ – 7.9 . The closest earthquake to the city center is the 1992 Orhanlı–Seferihisar (İzmir) earthquake that occurred 32 km away from İzmir. The earthquakes occurred in İzmir Region from 1900s to present are summarized together with their magnitudes in Table 1 (Regional Earthquake-Tsunami Monitoring Center (RETMC) 2021).

2.2 Seismic activity from October 30, 2020, to November 11, 2020

This earthquake occurred at 16.54 km depth is 23.38 km away from the Doğanbey Payımlı Village of Seferihisar District in İzmir City, which is the closest residential area. There were recorded 3550 aftershocks with varying magnitudes between 1.0 and 5.1 after the main shock up to the date 11.11.2020. While 55 of these aftershocks had the magnitude value of $M_w > 3$, the actual earthquake duration has been determined as 15.68 s according to the initial measurements (AFAD 2021).

3 Evaluation of ground motion

According to the pre-evaluation results performed with 129 accelerometers, the largest acceleration was measured as 179.31 gal in the north–south component of the No. 0905 accelerometer station. The acceleration values recorded by the closest 10 accelerometer stations to the epicenter of the earthquake are given in Fig. 5, while the information about the stations is given in Table 2. The acceleration records in the north–south, east–west



Fig. 4 Active fault map of İzmir Region (RETMC 2021)

Table 1 Historical Izmir earthquakes and magnitudes

Date	Time	Latitude	Longitude	Depth (km)	Distance to Izmir (km)	Magnitude	Location
09.08.1912	01:29:00.00	40.60	27.20	16	242	7.3	ERIKLICE-SARKOY (TEKIRDAG)
18.11.1919	21:54:50.30	39.26	26.71	10	100	7.0	KUCUKKOY-AYVALIK (BALIKESIR)
26.06.1926	19:46:38.80	36.54	27.33	100	209	7.7	DODECANESE (MEDITERRANEAN SEA)
31.03.1928	00:29:48.90	38.18	27.80	10	64	6.5	DEREBASI-TIRE (IZMIR)
22.09.1939	00:36:36.60	39.07	26.94	10	74	6.6	KIZILCUKUR-DIKILI (IZMIR)
13.12.1941	06:16:05.30	37.13	28.06	30	165	6.5	DAGPINAR (MUGLA)
06.10.1944	02:34:48.70	39.48	26.56	40	128	6.8	EDREMIT GULF (AEGEAN SEA)
23.07.1949	15:03:33.20	38.57	26.29	10	76	6.6	KUCUKBAHCE COASTAL ZONE (AEGEAN SEA)
18.03.1953	16:06:16.10	39.99	27.36	10	175	7.2	SOGUCAK-YENICE (CANAKKALE)
16.07.1955	07:07:17.00	37.65	27.26	40	86	6.8	YUVACA-SOKE (AYDIN)
09.07.1956	03:11:42.60	36.69	25.92	10	220	7.4	MEDITERRANEAN SEA
09.07.1956	03:24:09.10	36.59	25.86	40	233	6.5	MEDITERRANEAN SEA
06.10.1964	14:31:23.00	40.30	28.23	34	229	7.0	OKULAR-KARACABEY (BURSA)
04.03.1967	17:58:09.00	39.25	24.60	60	239	6.5	AEGEAN SEA
19.02.1968	22:45:42.40	39.40	24.94	7	220	7.1	AEGEAN SEA
28.03.1969	01:48:29.50	38.55	28.46	4	116	6.6	SOGANLI-ALASEHIR (MANISA)
28.03.1970	21:02:23.50	39.21	29.51	18	224	7.0	KIZIK-CAVDARHISAR (KUTAHYA)
27.03.1975	05:15:07.90	40.45	26.12	15	242	6.7	SAROS GULF (AEGEAN SEA)
19.12.1981	14:10:51.10	39.22	25.25	10	187	7.2	AEGEAN SEA
27.12.1981	17:39:13.30	38.91	24.92	10	201	6.5	AEGEAN SEA
20.07.2017	22:31:09.66	36.97	27.41	7.1	163	6.6	GOKOVA GULF (MEDITERRANEAN SEA)

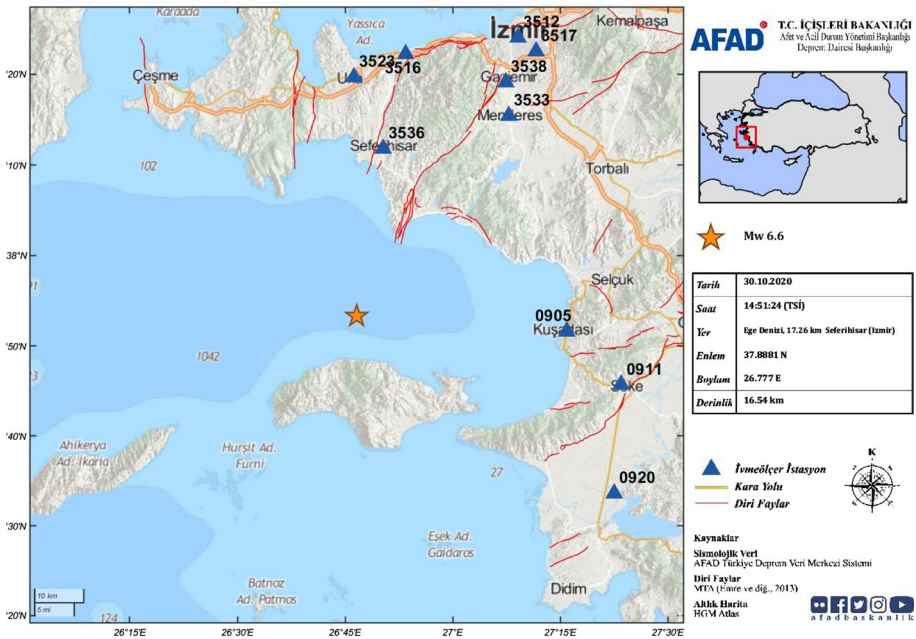


Fig. 5 The distribution of five closest accelerometer stations recording the earthquake (AFAD 2021)

Table 2 The accelerometer stations in the region and the measured acceleration values (AFAD 2021)

Station					Measured acceleration values (gal)			Distance, R_{epi}	$V_{s,30}$
Code	City	District	Longitude	Latitude	N-S	E-W	U-D	(km)	(m/s)
3536	İzmir	Seferihisar	26.83839	38.19681	50.22	79.14	31.31	34.75	1141
0905	Aydın	Kuşadası	27.26501	37.85997	179.31	144.02	79.84	42.95	369
3523	İzmir	Urla	26.7706	38.3282	80.32	63.57	36.90	48.94	414
3533	İzmir	Menderes	27.13017	38.25717	73.64	45.90	37.46	51.38	415
3516	İzmir	Güzelbahçe	26.8907	38.3706	47.29	48.36	32.08	54.57	460
3538	İzmir	Gaziemir	27.123347	38.318703	85.48	76.95	39.26	56.67	–
3528	İzmir	Çeşme	26.37256	38.30393	117.57	149.31	77.00	58.23	532
3519	İzmir	Karşıyaka	27.1112	38.4525	150.09	109.97	34.17	69.23	131
3513	İzmir	Bayraklı	27.1671	38.4584	106.28	94.67	44.19	72.00	196
3526	İzmir	Menemen	26.97953	38.57823	88.77	81.50	29.15	78.75	205

and vertical directions of the horizontal and vertical ground motion acceleration records obtained from No.0905 Aydın–Kuşadası station are given in Fig. 6 (AFAD 2021). In addition, the design acceleration spectra comparisons for 5% damping ratio are given in Fig. 7 for the spectral acceleration values of Aydın–Kuşadası (0905) station by considering the Regulation on structures to be built in disaster areas-1975 (TEC 1975), Regulations on structures constructed in disaster regions-1997 (TEC 1998), Regulations on structures constructed in disaster regions (TEC 2007) and Specifications for Building Design Under

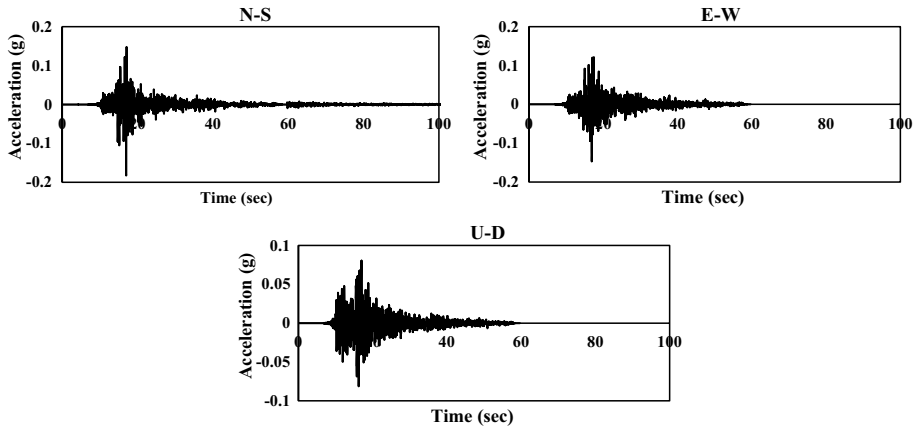
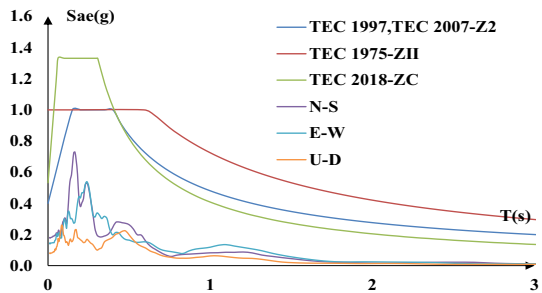


Fig. 6 The acceleration values of No.0905 Aydın–Kuşadası station

Fig. 7 The comparisons of design acceleration spectra according to the regulations



Earthquake Effects (TEC 2018). According to the Turkish Seismic Zone Map and Index adopted in 1996, İzmir Bayraklı District Center is located in the first-degree earthquake zone. The soil properties of Adalet, Manavkuyu and Mansuroğlu neighborhoods in which massive collapses and heavy damages were experienced are accepted as ZII, Z2, Z2 and ZC according to TEC-1975, TEC-1997, TEC-2007 and TEC-2018, respectively. Moreover, it is seen in the comparisons that the records taken at this station remained below all three design spectrums.

4 Damage of RC structures during the İzmir earthquake

The building stock constructed in Turkey before 2000 has been usually produced by cast-in-situ concrete. In addition to low concrete strength, unribbed and low-strength reinforcements have been used as the structural steel of the load-bearing structural members in the constructions. After 2000s, the increase in the number of the ready-mixed concrete facilities by the aid of the developing economy and technology has made the use of ready-mixed concrete widespread. Additionally, the use of high-strength ribbed reinforcement was obliged by the regulations. İzmir City located at the seaside with its dominant marine climate in general has RC buildings most of which belong to former building stock. Since sea sand has been usually used for the concrete production of these buildings constructed

with cast-in-situ concrete, one of the major defects of them is corrosion and carbonating. Moreover, there are some productions against zoning (floor addition contrary to project, conversion of ground floors into shops, etc.) in some of these old buildings. In general, since the ground floors of the buildings located on the main streets are designed as work-places, the height of the ground floors of most of these buildings is high with soft and weak floor irregularities. In the region, overhangs have been constructed to increase the building area at the upper floors. In Fig. 8, the typical building examples are shown in order to represent the building stock in İzmir.

4.1 Structural Damages and Causes of Failures

Detecting the structural damages by the aid of the site investigations made after the earthquakes, the earthquake regulations are updated and developed. The earthquake regulations in Turkey have been also updated for 4 times in last 50 years; TEC-1975, TEC-1997, TEC-2007 and the current one TEC-2018. In TEC-2008 regulations, the section of earthquake performance analysis for the existing buildings has been added. Furthermore, in TEC-2018, it has been obliged to make earthquake performance analysis for the new buildings to be built and to provide the earthquake performance targets with respect to the building importance factor. Besides all these, the spectrum values depending on the site-specific coordinates can be used instead of four different spectrum diagrams defined according to the degree of earthquake zone.

As a result of the site investigations made by the authors after the İzmir earthquake, it was seen that most of the heavily damaged or collapsed buildings have been designed in accordance with the TEC-1975 Regulation in terms of the year of construction. In the section of TEC-1975 related to the reinforced concrete buildings, there exist the definition of the minimum dimension and reinforcement details of the reinforced concrete members such as column, beam and shear wall and the principles for shear calculation of column-beam connection zones. However, it was seen in the construction site that the details in the regulation (not using stirrups at the column-beam joints, anchorage insufficiency in longitudinal beam reinforcement, large stirrup spacings, stirrups with 90 degree hooks, stirrup confinement, etc.) were not applied and the on-site inspection could not be provided sufficiently. These non-ductile frames formed as a result of these insufficiencies in practical have shown their effects on both completely/partially



Fig. 8 Typical RC building in İzmir region (images by authors)

collapsed and heavily damaged buildings during the last earthquake (IMO 2020). On the other hand, in some new high-rise buildings, heavy damages on the partition walls were also observed.

4.1.1 Soft story–weak story

The information determined by the investigations performed on the heavily damaged buildings in the İzmir earthquake has showed that these buildings had non-ductile reinforced concrete frames. Since the ground floors of the buildings on the main street were designed as workplaces, the height of the ground floor of most of the buildings is high with soft and weak story irregularities. Glass walls were used instead of the infill walls at the ground floors since the buildings were used as workplaces, which affects the non-ductile frames' strength and stiffness between the floors resulting in the danger of sudden collapse of the buildings. For the buildings with infill walls, the infill walls are only considered in the vertical load effect, and additionally they gain lateral drift stiffness to the buildings by protecting their completeness up to a definite level of earthquake force. In an analytical model with soft and weak story irregularity according to the acceleration records of İzmir earthquake, the removal of the infill walls at the ground floors increased the ground floor drift ratio of the building by 12.5 times (Koçer et al. 2018a, 2018b). Accordingly, hinges occur at the column ends of the ground floor of the building without any damage at the upper floors, and the load-carrying capacity of the building decreases. Thus, the building cannot absorb the accumulated earthquake energy by presenting a non-ductile behavior. In Fig. 9, some buildings having no infill wall but soft story mechanism at the ground floors can be seen with large plastic deformations developed at the ground floor column ends.

In the light of the information obtained from the previous earthquakes, some improvements related to the infill walls were made in TEC-2018. For instance, two different relative story drift ratio formulations have been presented according to the infill walls' jointed or jointless connection to the reinforced concrete frame. Here, the relative story drifts of the partition walls formed with jointless connection have been limited by reducing two times in comparison with the partition walls formed with jointed connections.



Fig. 9 The building examples damaged due to weak and soft story irregularity (image by authors and (AFAD 2021))

4.1.2 Column-Shear Wall

The lap splices were at the lower and middle regions of the columns according to TEC-2007 and earlier regulations that the lap splice length was required to be the same as the coupling length (Eq. 1) (TS 500–2000 2000) if it is at the middle and 1.5 times of the coupling length if it is at the lower region. According to TEC-2018 Regulation, the lap splice is allowed only at the middle region of the column. At these regions, stirrup confinement is compulsory in both regulations. The site observations in the earthquake area showed that the stirrup confinements have not been applied on the columns in accordance with the regulations. Furthermore, it was seen for the lap splices applied at the middle regions of the columns, if the stirrup confinement was not made with appropriate rate and length, buckling occurred in the longitudinal reinforcement at the lower end of the lap splice due to the variation encountered in the axial stiffness of the column (Fig. 10.a). In Fig. 10.b, a reinforced shear wall designed as shear wall and damaged during the earthquake is shown. The ribbed reinforcement was used at the shear wall boundary zones, while unribbed reinforcement at the middle regions. In addition, no stirrups were used in the shear wall boundary zones, and unribbed and hookless stirrups were used in the whole shear wall cross-section. Moreover, the lap splices at the longitudinal reinforcements of the shear wall were produced at the middle region of the shear wall, and no stirrup confinement was made. For this reason, damage is concentrated at the lap splice region during the earthquake, and the lap splices in this region were stripped.

$$l_b = \left(0.12 \times \frac{f_{yd}}{f_{ctd}} \times \emptyset \right) \geq 20\emptyset \tag{1}$$

In Fig. 11, the damages that occurred at the columns in which stirrup confinement has not been done at the lower region of the column were pictured, which were frequently met during the investigations carried out in the earthquake region. Not having any detailing of the reinforced concrete members according to TEC-1997 Earthquake Code is the common feature of these damaged buildings. The damage levels were high due to unribbed reinforcement and poor quality concrete production for the longitudinal reinforcements. In addition, the stirrup confinement and hookless horizontal reinforcement production caused

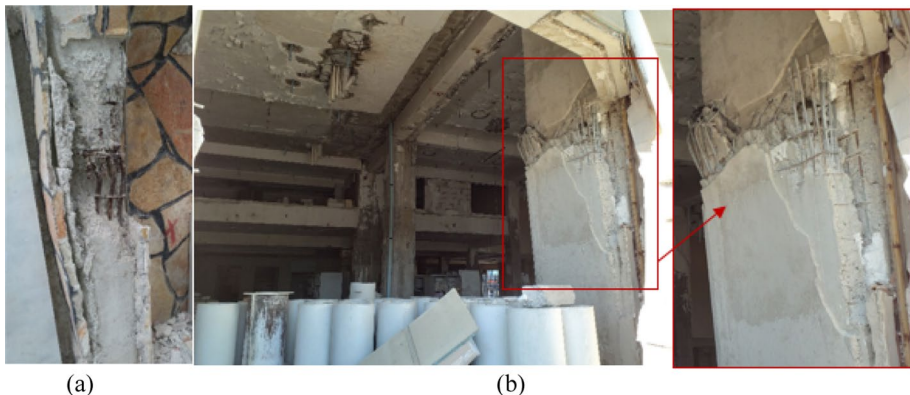


Fig. 10 Column and shear wall damages (image by authors and (AFAD 2021))



Fig. 11 Column damages (image by authors and (AFAD 2021))



Fig. 12 Secondary beam damages (image by authors and (AFAD 2021))

the unfastening and then buckling of the longitudinal reinforcement; corrosion damage occurred due to the concrete quality and caused the coupling unfastening in the members.

4.1.3 Beam

While examining the earthquake damages on the reinforced concrete buildings, besides the hinging formation at the beams due to the lateral effect of earthquake, the vertical earthquake effects that are not so much considered in building design also causes various damages on the buildings. Due to the vertical earthquake effect of İzmir earthquake, some of the buildings with long beam spans faced with cracks which usually occurred at the center points of the beams where more bending takes place (Fig. 12.a). On the other hand, in some buildings due to the architectural reasons, the secondary beams can be made which starts from a column and connected to a beam with no column or not starting from a column but placed between two beams vertically. When the lateral earthquake forces affect the building, the secondary beams transfer loads from the nodal points they are connected to the main beams; in this case, this means a single load acting from nodal point to the main beam that can cause damages at these regions. Since there is no restriction about the secondary beams in current and former regulations in Turkey, the construction of this type of beams in buildings still continues. In Fig. 12.b,c., some of the damages that occurred on the main beams due to secondary beams in İzmir earthquake are shown.

4.1.4 Column-beam connection zone

One type of the widespread damages experienced in the İzmir earthquake was the damages observed at the column-beam connections (Bursa Technical University 2020). The main reason of these damages was not keeping the installation of stirrups throughout the column length at the column-beam connection zone. The provision and details of stirrup application at the column-beam connections have been explained comprehensively in all the today's and past regulations. According to TEC-1975 regulations, the amount of stirrups applied for the unit length of the column-beam connection zone should not be less than the amount of stirrups applied for the unit length of the middle zone of the column. There were two conditions in question for the confined and unconfined column conditions in TEC-1997, TEC-2007 and TEC-2018 regulations. In confined connections, at least 40% of the amount of stirrups existing at the confinement zone of the lower column will be used throughout the connection zone. However, the diameter of the stirrup will not be less than 8 mm, and their spacings will not exceed 150 mm. In the unconfined connections, at least 60% of the amount of stirrups existing at the confinement zone of the lower column will be used throughout the connection zone. Here, the diameter of the stirrup will not be less than 8 mm, and their spacings will not exceed 100 mm. Despite the provisions about the column-beam connection zones defined in all these regulations, the requirements for these regions have not been applied in most of the buildings. Since stirrups have not been used in column-beam connection zones, damages are concentrated at these regions. Furthermore, due to the lateral stiffness of beam larger than the lateral drift stiffness of column, the damages were concentrated at the column-beam joints during the lateral load transfer to the columns together with the lateral effect of the earthquake. In order to avoid the possible shear forces that can occur due to this reason, stirrups should be applied to the column-beam connection zones and possible damages should be prevented. Since no stirrups have been used at the column-beam connection zones of some buildings, during the İzmir earthquake, the longitudinal reinforcements at these zones were buckled and columns lost their load-bearing capacities (Fig. 13 a,b,c). In addition to this, it is a possible condition that the width of the beam is less than the width of the column at the nodal point at which the beam is connected to the column. Also under this condition, the stirrup application should continue throughout the column. However, as seen in Fig. 13d, this condition has not been taken into consideration in some buildings, and the buckling of the longitudinal reinforcement of the columns caused damages at the column-beam connection zones.



Fig. 13 Column-beam connection zone damages (image by authors and (AFAD 2021))

4.1.5 Strong beam–weak column

The energy of the earthquake should be consumed by various mechanisms in destructive earthquakes. For instance, the hinging is desired to occur at the beam ends in order to provide the building to consume the energy of the earthquake by presenting a ductile behavior during the earthquake. For this reason, today's construction regulations include some conditions for plastic hinges to occur at the beams instead of columns. The most important one of them is that the sum of the moments of the load-carrying capacity of the columns connected at each column-beam nodal point should be at least 20% greater than the sum of the moments of the beam cross-sections' load-carrying capacity obtained on the column face at the same nodal point. In many of the buildings collapsed or heavily damaged in the earthquake occurred in İzmir on October 30, 2020, the floors were collapsed one on the top of the other just like a pancake due to strong beam–weak column production besides the low lateral drift stiffness (Fig. 14a). The strong beam–weak column damages experienced in the İzmir earthquake are shown in Fig. 14b, c

4.1.6 Infill Wall damage

As seen in Fig. 15, during the earthquake, no damage was observed on the reinforced concrete frame system of the building designed in ductile shear wall + frame system according to TEC 2007 Earthquake Code. This building is located in the Bayraklı District where the buildings collapsed or heavily damaged during the İzmir earthquake were concentrated. The building with its ductile load-bearing system contributed against the earthquake loads during the oscillations of the earthquake due to the contribution of walls to the lateral drift stiffness. However, this building that can be considered as luxury category in terms of building usage quality faced with partition wall damage that cannot be expected in this level of earthquakes. Hence, it is concluded that the aforementioned building had insufficient drift controls in the design or insufficient amount of shear wall cross-sectional areas (Fig. 15).

4.1.7 Overhangs

The effect of vertical earthquake acceleration on the buildings is considerably less when compared to the lateral earthquake acceleration. In addition, the load-carrying system members against the vertical load are accepted to remain in the safe side due to the parameters such as material, load coefficient and axial load level. However, damages occur during



Fig. 14 Strong beam–weak column formation (image by authors and (AFAD 2021; TEC 2018))

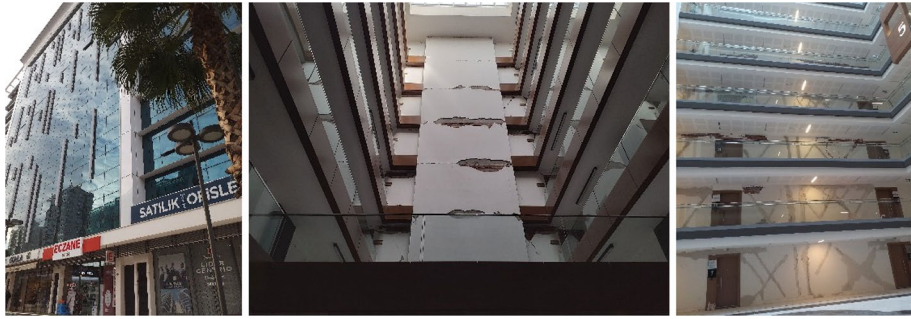


Fig. 15 Infill wall damage (image by authors and (AFAD 2021))

the earthquakes on the overhangs of the buildings due to the vertical earthquake acceleration depending on the lengths of the overhangs. Owing to the damages occurred on the overhangs during the previous earthquakes, various studies were carried out and vertical acceleration spectrum was firstly included to the current earthquake regulation (TEC 2018; Arslan et al. 2013; Tan et al. 2008; Inel et al. 2013). According to the current regulation, the vertical earthquake analysis became obligatory for the beam members exceeding 5 m cantilever span or 20 m horizontal span. For the buildings not having the above-mentioned problems, the vertical earthquake acceleration is taken into consideration by adding the 2/3 ratio of the short-period horizontal acceleration to the dead load. The observed earthquake damages occurred at the overhangs constructed for architectural concerns during the İzmir earthquake are shown in Fig. 16. The overhang walls of the damaged buildings were separated from the main frame or fell down from the out-of-plane facade.

4.1.8 Secondary Beam

One of the damages caused by horizontal and vertical earthquake acceleration in structures is secondary beam damage. This structural defect, which is generally seen in buildings, was also observed in the on-site investigations after the earthquake in İzmir. The effect of the high-order shear force in the secondary beam region and the vertical dynamic effect caused the shear damage to intensify in the beam with low stiffness. Photographs of this damage are given in Fig. 17. As it can be seen in Fig. 17, the cracks in the beams with a greater span from the main beam on which the secondary beam rests extended to the slab. While the magnitude of the horizontal acceleration to which the structures are exposed during the earthquake is in the order of 0.179 g, the magnitude of the vertical acceleration is almost half (0.08 g). Since this vertical effect is also considerably high, it caused such damages to both the overhangs and the secondary beams in the buildings.

4.1.9 Staircase

In reinforced concrete structures, with the assumption of rigid diaphragm, the horizontal load is distributed to the vertical load-bearing elements by the slabs. In areas where there are floor discontinuities such as stairwells, such damages are seen because the horizontal load cannot be transferred to other floors due to the semi-rigid diaphragm behavior. Due to such effects, damage occurs in the support areas of the stairs manufactured



Fig. 16 Overhang damages (image by authors and (AFAD 2021))

with simple support. Since the tension in the support region is on the upper side, if the compression region is not sufficiently equipped, tensile stresses occur in these regions during earthquakes and such damages are observed. This type of damage is shown in Fig. 18. As can be seen from these photographs, structural damages generally occurred at the bottom of the area where the staircase was supported on the slab.



Fig. 17 Secondary beam damages (image by authors and (AFAD 2021))

4.1.10 Corrosion

Corrosion is one of the basic problems of the buildings existing in the marine climate regions. Corrosion damage was observed in general of the buildings damaged in the İzmir earthquake. The common features of the buildings faced with corrosion damage are poor quality concrete class, concrete cover insufficiency or carbonating problem arising from the use of aggregate and sand obtained from sea in the concrete production. Since one of the primary reasons of the corrosion formation at the reinforced concrete members is the carbonation of the concrete, the depth of carbonation should be measured. In this study, concrete samples and core samples were taken from a representative building and carbonation depths were measured, because the reason for some of the damages occurred in İzmir earthquake was thought to be corrosion. The concrete specimens taken from the columns of the aforementioned building were cut, and their surfaces were cleaned. Then, the carbonation depth was determined by spraying phenolphthalein indicator on the cut and cleaned concrete specimens. After the phenolphthalein indicator comes into contact with the concrete surface, the color of the non-carbonated concrete surfaces turns into purple while carbonated concrete surfaces show no color change. In Fig. 19, the carbonation depth was measured by taking the concrete cover layer from the representative building in İzmir Bayraklı Region and cutting the cover layer in the direction of the cross-section. As seen from the figure, entire section except a few number of spots has been carbonated, and carbonation has become effective in the entire concrete cover. The reinforcements of this column have been corroded, and their cross-sections have been considerably decreased due to carbonation effect.



Fig. 18 Staircase damages (image by authors and (AFAD 2021))

Furthermore, the carbonation depth for the core sample obtained from the representative building was measured, and similarly the carbonation effect on the entire core sample was observed. After the compression test applied on the core sample, a low strength value of 14.6 MPa was obtained, since the entire cross-section was completely affected from the carbonation depth (200 mm). Similar results for the relationship between the compressive strength of concrete and carbonation were also obtained in the related studies (Khan and Lynsdale 2002; Kim et al. 2009). The pictures of the buildings faced with corrosion damages are given in Fig. 20.

5 Case Study

As a result of the on-site investigations after the İzmir earthquake, it was observed that a building in Bayraklı District designed in 1998 as a 3-story building but constructed in-site as 5-story by adding two more floors. Although this building has been constructed in a highly destructive region during the İzmir earthquake and the static modeling of the

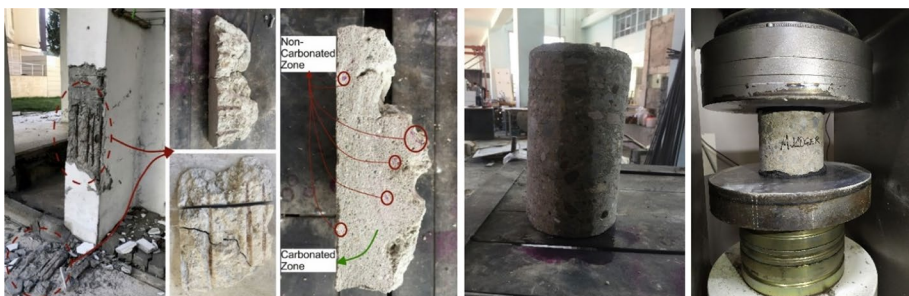


Fig. 19 Determination of carbonation depth and core compression test



Fig. 20 Corrosion damages (image by authors and (AFAD 2021))

building was made as 3-story, it has survived the earthquake by satisfying the immediate occupancy performance level without any permanent damage; this is because the concrete class was above the standards according to that time conditions, the reinforcements used in columns and beams were applied in accordance with all the reinforcement provisions in TEC-1997, the column-beam details were constructed in appropriate to the regulations, the building was formed in accordance with the project. Therefore, the building was modeled in 3D in accordance with its static project by the aid of the ETABS finite elements program, and nonlinear time-history analysis, pushover analysis and linear analyses were made according to the acceleration records of İzmir earthquake. Additionally, the linear analyses of the building were performed according to the earthquake code valid in the construction year and today's current earthquake code.

5.1 Brief description of the selected existing RC buildings

The existing building considered in the case study is located at the Bayraklı District of İzmir City, which consists of a basement floor three sides surrounded with shear walls, a ground floor and 4 typical floors. The exterior view of the building constructed in 1998 is given in Fig. 21. The load-bearing system of the building has been formed with reinforced concrete frames, and the floor system has been produced with beam-reinforced concrete plate where the slab thickness was 120 mm. Except the shear walls at the basement floor, there was no shear wall in the construction. The cross-sectional dimensions of the columns

were $250 \times 500 \text{ mm}^2$, $250 \times 600 \text{ mm}^2$, $250 \times 700 \text{ mm}^2$ while all the beams of the building in $250 \times 500 \text{ mm}^2$ dimensions. Being constant in the whole building the floor height is 2700 mm. All the static properties and details of the building were taken from the existing static project whose details are given in Fig. 22. In order to determine the concrete compressive strengths of the existing vertical load-bearing elements, the non-destructive strength determination was made by using Schmidt hammer in many columns. The concrete compressive strength of the existing building was C25 (25 MPa) that similar results were also obtained according to the Schmidt hammer test. In addition, the yield strength of the reinforcement used for the construction of the building was taken as S220 (220 MPa) in appropriate to the existing static project. Soil class is Z4, which is similar to class D soil in FEMA-356 (FEMA-356 2000). TEC-1997 specifies spectrum characteristic periods as 0.20 s and 0.90 s in this type of soil.

5.2 Analytical model

The three-dimensional modeling and the nonlinear analyses of the reinforced concrete building were performed by ETABS computer program, and the modeled building's three-dimensional view is shown in Fig. 23.

In the ETABS program, columns and beams are modeled as bar elements. To account for nonlinear behavior, the plastic hinges' properties described in FEMA-356 are defined for the end regions of the column and beam members where the inelastic deformation is dense. Plastic hinges with a length of $0.5 H$ were assigned to the zones to reach their capacity under the changing internal force distribution (Arslan and Korkmaz 2007; Murat 2015). Figure 24 shows the internal force–deformation diagram of an idealized plastic hinge and points corresponding to performance levels. Once the plastic hinges' properties are defined, the static load is increased step by step until the samples' failure. Pushover analysis was performed with displacement control. Performance levels



Fig. 21 The current view of the modeled building

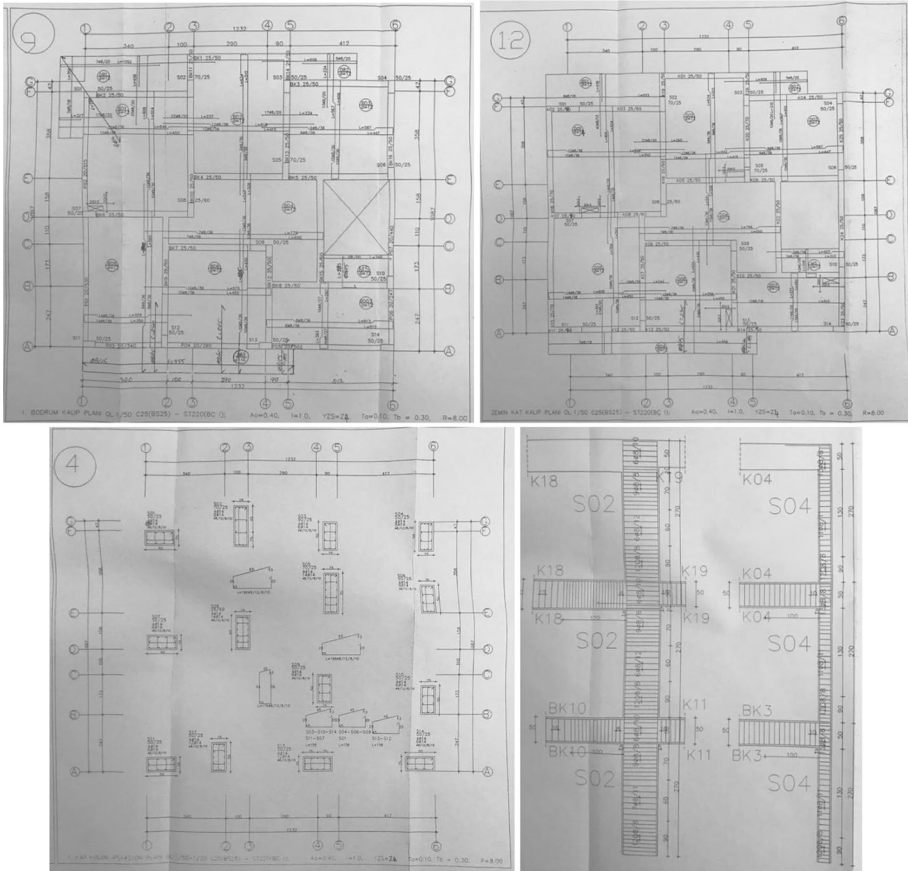


Fig. 22 Static projects of the modeled building

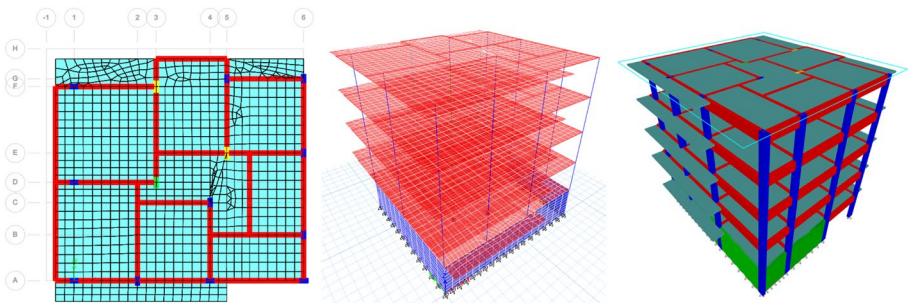


Fig. 23 Three-dimensional ETABS model of the building

are composed of immediate occupancy (IO), life safety (LS) and collapse prevention (CP). In Fig. 24, point B refers to the point of yield and point E refers to the point of section collapse. In the analysis, P- Δ effect was taken into account. Also, no additional eccentricity was applied to the building, the elastic earthquake load reduction coefficient

was taken as $R = 1$, and the rigid regions were defined to the beam and column ends by the program in accordance with TEC-2018.

5.3 Analytical results

5.3.1 Nonlinear static pushover analysis results

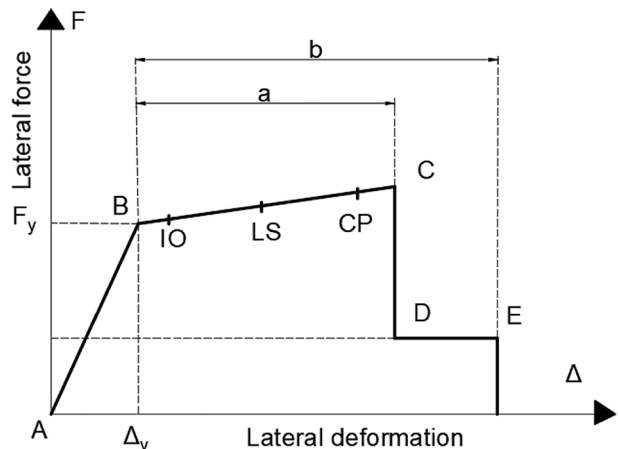
After the modeling, the performance of the building was determined according to TEC-2018 regulations. The base shear force-top displacement curve for nonlinear procedures was converted into spectral displacement-spectral acceleration curve in Fig. 25. The nonlinear displacement capacity of the building required during the earthquake was determined by defining the S_d value at the point where the tangent drawn to the initial curves of the capacity curves of the building in X and Y directions cut the spectrum curve. The reference design spectrum here was taken into account for the design earthquake with 10% probability of exceedance in 50 years according to the 2018 Earthquake Regulation. The elastic spectrum curve in Fig. 25 is the elastic design spectrum for the ZD soil class defined for the İzmir Region in TEC-2018. The top displacement request of the building in both directions was determined according to TEC-2018 from Eqs. 2 and 3 by the aid of the nonlinear elastic spectral displacements.

$$u_{xN1} = \phi_{xN1} \times \Gamma_{x1} \times d_1 = 0.0426 \times 29.698 \times 0.09442 = 0.11946\text{m} \tag{2}$$

$$u_{xN1} = \phi_{xN1} \times \Gamma_{x1} \times d_1 = 0.0245 \times 52.048 \times 0.07076 = 0.09023 \text{ m} \tag{3}$$

The plastic hinges occurred on the structural members of the building during the top displacement request obtained for the design spectrum are given in Fig. 26, and the plastic hinge damage levels at the column and beams corresponding to the top displacement request in Fig. 27. According to the pushover analysis results of the building in the X direction, 103 of 140 columns (73.57%) had no damage, 32 (22.85%) had minor damage, 4 (2.85%) had severe damage, and 1 column (0.71%) fell within the collapse region. In addition, according to the pushover analysis results in the Y direction, 79 of 140 columns

Fig. 24 Plastic hinge assignment and load deformation relation of plastic hinge (Arslan and Korkmaz 2007)



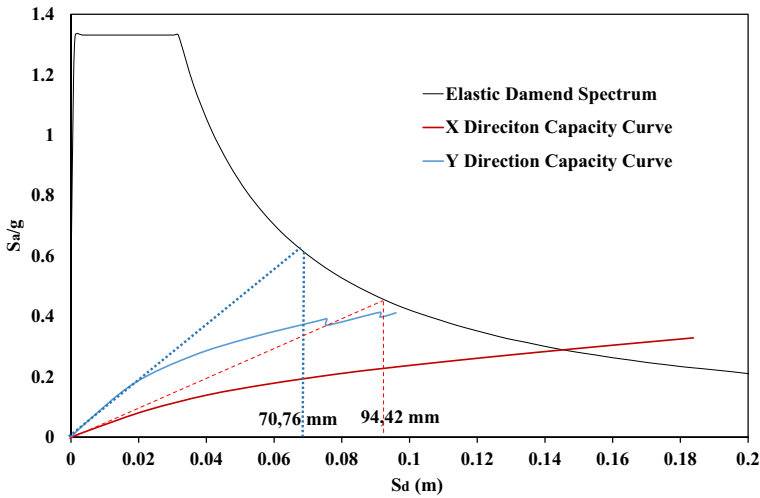


Fig. 25 Spectral displacement–spectral acceleration curve

(56.42%) had no damage, 51 (36.42%) had minor damage, 6 (4.28%) had severe damage, and 4 columns (2.85%) fell within the collapse region.

5.3.2 Nonlinear time history pushover analysis results

The shear force-top displacement hysteresis curves obtained by the nonlinear time-history pushover analysis performed in both directions of the building are given in Fig. 28. In addition, the maximum base shear forces obtained by time-history pushover analysis were calculated as 640 kN and 166 kN in X and Y directions of the building, respectively. When the building was designed as 3-story according to the 1998 regulation, the reduced design earthquake load was taken into consideration as 735.75 kN in the X direction and

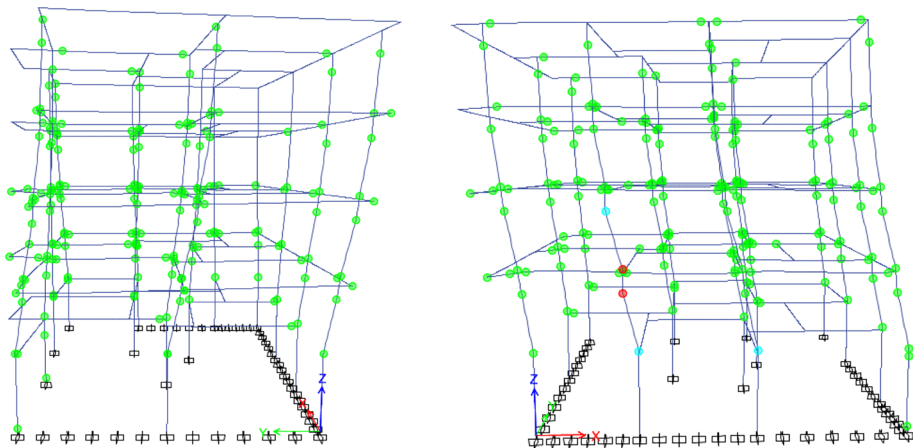


Fig. 26 Plastic hinges occurred in the building

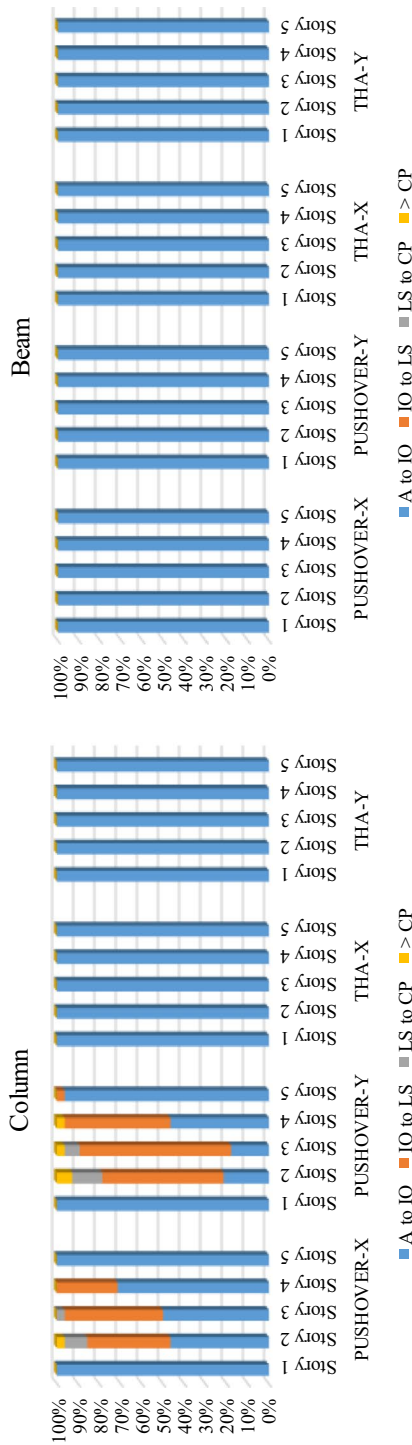


Fig. 27 Plastic hinge damage levels occurred at the columns and beams

896.75 kN in the Y direction; but if designed as 5-story according to TEC-2018, the current reinforced concrete construction regulation, the reduced design earthquake load would be determined as 614.137 kN and 627.23 kN in X and Y directions, respectively. Here, it is seen that the design earthquake load obtained depending on the building’s mass and period in the constructed year is greater than the base shear force occurred during the İzmir earthquake, and furthermore, with its current form it is considerably closer to the design earthquake load obtained by the current design spectrum. For this reason, the building survived the İzmir earthquake with elastic deformations without any permanent damages on the load-bearing system members. As seen in Fig. 28.a and b, the time-history hysteresis curve of the building is considerably low in comparison with the static pushover curve and remains in the elastic region of the pushover curve.

The plastic hinges occurred at the structural members during the nonlinear time-history analysis of the building performed according to the İzmir Earthquake acceleration record are shown in Fig. 29, and the plastic hinge damage levels at the columns and beams in Fig. 27. According to the THA results, in the X direction of the building, no damage occurred in 139 of the 140 columns (99.28%) and minor damage in 1 of them (0.72%); in the Y direction of the building, no damage occurred in 135 of the 140 columns (96.43%) and minor damage in 5 of them (3.57%).

6 Conclusions

The last destructive earthquake in Turkey was on October 30, 2020, the epicenter of the earthquake was the Aegean Sea, 17.26 km off the coast of Seferihisar (İzmir), the İzmir earthquake with a magnitude of $M_w = 6.9$, resulted in 117 casualties and 1032 injuries. The on-site observations and the results obtained by the case study can be listed generally as in the following;

- According to the acceleration records of İzmir earthquake, the recorded peak ground acceleration (PGA) was observed as nearly 0.182 g that this value is considerably less when compared to the elastic design spectrum diagram values (according to the design earthquake with 10% probability of exceedance in 50 years, and 475 years of return period) given in both TEC 1997 and current regulations for İzmir City.

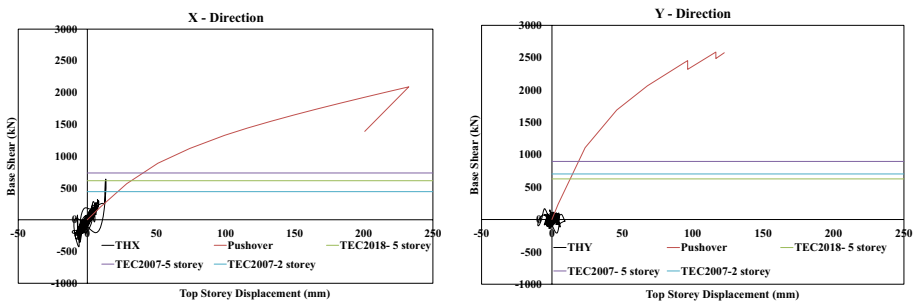


Fig. 28 Base shear force-top displacement hysteresis diagrams according to nonlinear time-history pushover analysis

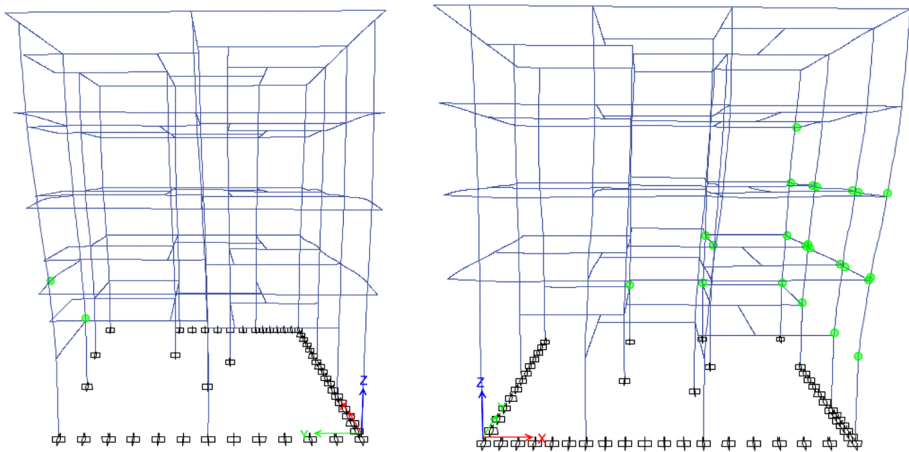


Fig. 29 Plastic hinges occurred at the structural members during the nonlinear time-history analysis

- The design earthquake, a light magnitude earthquake in comparison with the spectral acceleration values, caused more damages than expected due to the structural defects of the reinforced concrete buildings, and the duration of the earthquake was also very short (15.68 s).
- The spectral acceleration value of the building modeled in the case study was obtained as 0.44 g from the design earthquake with respect to the natural predominant period. This value remains in the safe side when compared with the peak ground acceleration value exposed to the building during the earthquake.
- The overstrength factor of the building considered in the case study was obtained as 2.84 and 2.87, respectively, in the X and Y directions. The overstrength factor is proposed as 1.5 according to TEC-1997 Regulation.
- When the capacities in both directions of the building were compared, the base shear forces of the considered building obtained from the nonlinear THA showed 3.66 and 15.66 times higher safety, respectively, for the X and Y directions. As can be seen, the building survived the İzmir earthquake by providing human life safety, since the structural capacity of the building in both directions remained in the safe side with respect to the lateral load exposed during the earthquake.
- The building considered in the case study was designed as one basement floor + 2 normal floors in the year of construction, and 2 more floors were added in the following years without any strengthening process. Despite this high degree of structural defect, in parallel to the nonlinear THA results the building has achieved the performance target of immediate occupancy during the earthquake due to the on-site detailing of the structural load-bearing elements in accordance with the project and the quality of concrete higher than the concrete class in the regulation at the time of construction which had good quality workmanship. If such a building having this kind of a significant structural defect can safely survive the earthquake both analytically and physically, it is obvious that collapsed or heavily damaged buildings lack significant control mechanisms.
- As a result of on-site investigations made after the İzmir earthquake, the structural and non-structural deficiencies such as the use of cast-in-situ poor concrete, the use

of unribbed low-strength reinforcement bars, the inappropriate production of RC elements' reinforcements according to the project, the carbonation and corrosion damages due to the use of sea sand, the design of the buildings inconsistent to the earthquake-resistant design philosophy (architectural cantilever, secondary beam, soft and weak story irregularities, nodal points with strong beam-weak column, etc.) were detected.

In general, the heavily damaged or collapsed buildings have been constructed before the regulations of TEC-1997, and all of them had similar structural deficiencies that caused similar structural damages. It has been observed that the buildings constructed after the 2000s generally met the life safety performance target during the earthquakes. By the aid of the developing technology after these years, the quality of the building stock has increased and the production of earthquake-resistant structures has been provided due to the availability of ready-mixed concrete facilities, the developments in the control mechanism and the tight control of the construction stages of the buildings. However, it is necessary to identify and examine the old building stock as soon as possible, which was constructed without any control, to perform the earthquake performance analyses, to detect the defects and to apply the appropriate strengthening.

Funding The authors declare that no funds, grants, or other support were received during the preparation of this manuscript. The authors have no relevant financial or non-financial interests to disclose.

Declarations

Conflict of interest The authors have no relevant financial and non-financial to disclose.

References

- Adalier K, Aydingun O (2001) Structural engineering aspects of the June 27, 1998 Adana-Ceyhan (Turkey) earthquake. *Eng. Struct.* 23:343–355. [https://doi.org/10.1016/S0141-0296\(00\)00046-8](https://doi.org/10.1016/S0141-0296(00)00046-8)
- AFAD (2021) Disaster and Emergency Management, (n.d.). <http://www.afad.gov.tr>
- Akkar S, Azak T, Çan T, Çeken U, Tümsa MD, Duman TY, Kale Ö (2018a) Evolution of seismic hazard maps in Turkey. *Bull Earthq Eng* 16:3197–3228
- Akkar S, Kale Ö, Yakut A, Ceken U (2018b) Ground-motion characterization for the probabilistic seismic hazard assessment in Turkey. *Bull Earthq Eng* 16:3439–3463
- Akkar S, ErogluAzak T, Çeken CU, Demircioğlu MB, Duman T, Kartal RF (2014) Türkiye Sismik Tehlike Haritasının Güncellenmesi. UDAP-Ç-13–06. In: Ulusal Deprem Araştırma Programı; Disaster and Emergency Management Presidency Press, Ankara
- Arslan MH, Korkmaz HH (2007) What is to be learned from damage and failure of reinforced concrete structures during recent earthquakes in Turkey? *Eng Fail Anal* 14:1–22. <https://doi.org/10.1016/j.engfailanal.2006.01.003>
- Arslan MH, Olgun M, Köroğlu MA, Erkan IH, Köken A, Tan O (2013) 19 May 2011 Kütahya-Simav earthquake and evaluation of existing sample RC buildings according to the TEC-2007 criteria. *Nat Hazards Earth Syst Sci* 13:505–522. <https://doi.org/10.5194/nhess-13-505-2013>
- Bursa Technical University (2020) 30 October 2020 Aegean Sea Openings M6.6 Earthquake Building Preliminary Assessment Report, Bursa
- Buyuksarac A, Isik E, Harirchian E (2021) A case study for determination of seismic risk priorities in Van (Eastern Turkey). *Earthq Struct* 20(4):445–455
- Çağatay IH (2005) Experimental evaluation of buildings damaged in recent earthquakes in Turkey. *Eng Fail Anal* 12:440–452. <https://doi.org/10.1016/j.engfailanal.2004.02.007>
- Chaoxu X, Gaozhong N, Huayue L, Xiwei F, Rui Y, Xun Z (2021) Comparative analysis of the earthquake disaster risk of cities in Eastern China based on lethal levels—a case study of Yancheng City. *Suqian*

- City and Guangzhou City, *Geom, Nat Hazards and Risk* 12(1):3224–3264. <https://doi.org/10.1080/19475705.2021.2009580>
- Doğangün A (2004) Performance of reinforced concrete buildings during the May 1 2003 Bingöl Earthquake in Turkey. *Eng Struct* 26:841–856. <https://doi.org/10.1016/j.engstruct.2004.02.005>
- Earthquake Zoning Map of Turkey (1996) General Directory of Disasters Adairs Press, Ankara, Turkey
- EMSC, European-Mediterranean Seismological Centre (2021). <https://www.emsc-csem.org/#2>.
- Gross LT, Phan JL (2000) Implications for earthquake risk reduction in the United States From the Kocaeli, Turkey, Earthquake of August 17, 1999, USGS Report
- Gülkan P, Kocyyigit A, Yüçemen M, Doyuran V, Basöz N (1993) En son verilere gore hazırlanan Türkiye Deprem Bölgeleri Haritası; ODTÜ Deprem Muhendisligi Arastırma Merkezi: Ankara, Turkey, pp 93–101
- IMO, Chamber of Civil Engineers Izmir Branch, İzmir Earthquake Report, İZMİR (2020). https://izmir.imo.org.tr/resimler/dosya_ekler/aff3f23a5bdfa1b_ek.pdf?tipi=2&туру=X&sube=16
- Inel M, Ozmen HB, Bilgin H (2008) Re-evaluation of building damage during recent earthquakes in Turkey. *Eng Struct* 30:412–427. <https://doi.org/10.1016/j.engstruct.2007.04.012>
- Inel M, Ozmen HB, Akyol E (2013) Observations on the building damages after 19 May 2011 Simav (Turkey) earthquake. *Bull Earthq Eng* 11:255–283. <https://doi.org/10.1007/s10518-012-9414-3>.
- Işık E, Büyüksaraç A, Ekinci YL, Aydın MC, Harirchian E (2020) The effect of site-specific design spectrum on earthquake-building parameters: a case study from the Marmara Region (NW Turkey). *Appl Sci* 10(7247):1–23. <https://doi.org/10.3390/app10207247>
- Kaplan H, Yılmaz S, Binici H, Yazar E, Çetinkaya N (2004) May 1, 2003 Turkey - Bingöl earthquake: Damage in reinforced concrete structures. *Eng Fail Anal* 11:279–291. <https://doi.org/10.1016/j.engfailanal.2003.08.005>
- Khan MI, Lynsdale CJ (2002) Strength, permeability, and carbonation of high-performance concrete. *Cem Concr Res* 32:123–131. [https://doi.org/10.1016/S0008-8846\(01\)00641-X](https://doi.org/10.1016/S0008-8846(01)00641-X)
- Kim JK, Kim CY, Yi ST, Lee Y (2009) Effect of carbonation on the rebound number and compressive strength of concrete. *Cem Concr Compos* 31:139–144. <https://doi.org/10.1016/j.cemconcomp.2008.10.001>
- Koçer M, Öztürk O, Ünal A (2021a) Comparison of TEC 2018 and TEC 2007 according to İzmir Earthquake Acceleration Record, in: IES'20 Int. Eng. Symp., İzmir Democracy University, İZMİR, pp 127–132
- Koçer M, Ünal A, Öztürk O (2021b) Evaluation of TEC 2018 and TEC 2007 Regulations in the Buildings Having B1 and B2 Irregularities in accordance with İzmir Earthquake (31.10.2020), In: IES'20 Int. Eng. Symp., İzmir Democracy University, pp 133–138
- Murat O (2015) Field reconnaissance of the October 23, 2011, Van, Turkey, earthquake: lessons from structural damages. *J Perform Constr Facil* 29:04014125. [https://doi.org/10.1061/\(asce\)cf.1943-5509.0000532](https://doi.org/10.1061/(asce)cf.1943-5509.0000532)
- NOA, Institute of Geodynamics National Observatory of Athens (2021) İzmir Earthquake Report. <http://www.gein.noa.gr/en/>
- FEMA-356 (2000) Commentary for the seismic rehabilitation of buildings, Washington
- RETMC, Regional Earthquake-Tsunami Monitoring Center (RETMC) (2021). <http://www.koeri.boun.edu.tr/scripts/lst2.asp>.
- SAKOM (2020) Health Disaster Coordination Center, Disaster and Emergency Management. <https://deprem.afad.gov.tr/downloadDocument?id=2065>.
- Sezen H, Whittaker AS, Elwood KJ, Mosalam KM (2003) Performance of reinforced concrete buildings during the August 17, 1999 Kocaeli, Turkey earthquake, and seismic design and construction practice in Turkey. *Eng Struct* 25:103–114. [https://doi.org/10.1016/S0141-0296\(02\)00121-9](https://doi.org/10.1016/S0141-0296(02)00121-9)
- Shendkar MR, Kontoni DPN, Işık E, Mandal S, Maiti PR, Harirchian E (2022) Influence of Masonry Infill on Seismic Design Factors of Reinforced-Concrete Buildings, Shock and Vibration. 1–15. <https://doi.org/10.1155/2022/5521162>
- Tan O, Tapırdamaz MC, Yörük A (2008) The earthquake catalogues for Turkey, Turkish. *J Earth Sci* 17:405–418
- TEC (1975) Regulation on structures to be built in disaster areas, Regulations on structures constructed in disaster regions, Ankara, Turkey
- TEC (1998) Turkish Earthquake (Seismic) Code, Regulations on structures constructed in disaster regions, Ankara
- TEC (2007) Turkish Earthquake (Seismic) Code, Regulations on structures constructed in disaster regions
- TEC (2018) Turkish Earthquake Code: Specifications for Building Design Under Earthquake Effects, Regulations on structures constructed in disaster regions, Ankara

- TS 500–2000 (2000) Requirements for design and construction of reinforced concrete structures, Turkish Standards Institute
- Ulusay R, Kumsar H, Konagai K, Aydan Ö (2012) The characteristics of geotechnical damage by the 2011 Van-Erciş earthquake In: Proceedings of the international symposium on engineering lessons learned from the 2011 Great East Japan Earthquake, pp 1926–1937
- USGS (2021) The United States Geological Survey, Izmir Earthquake Report. <https://www.usgs.gov/>.
- Yurdakul Ö, Duran B, Tunaboyu O, Avşar Ö (2021) Field reconnaissance on seismic performance of RC buildings after the January 24, Elazığ-Sivrice earthquake. Nat Hazards 105:859–887. <https://doi.org/10.1007/s11069-020-04340-x>

Publisher's Note Springer Nature remains neutral with regard to jurisdictional claims in published maps and institutional affiliations.

Springer Nature or its licensor (e.g. a society or other partner) holds exclusive rights to this article under a publishing agreement with the author(s) or other rightsholder(s); author self-archiving of the accepted manuscript version of this article is solely governed by the terms of such publishing agreement and applicable law.